Available online at www.sciencedirect.com
ScienceDirect
Veterinary Immunology and Immunopathology 122 (2008) 204–215
Veterinary immunology and immunopathology
www.elsevier.com/locate/vetimm

Altered lymphocyte homeostasis after oral prion infection in mouse

F. Díaz-San Segundo [a,1], N. Sevilla [a], J.P. Gutiérrez [b], A. Brun [a,*]

[a] *Centro de Investigación en Sanidad Animal (CISA-INIA), Carretera de Algete a El Casar km 8,100, Valdeolmos 28130, Madrid, Spain*

[b] *Departamento de Producción Animal, Facultad de Veterinaria, Universidad Complutense de Madrid, Avda. Puerta de Hierro s/n, 28040 Madrid, Spain*

Received 2 May 2007; received in revised form 26 November 2007; accepted 30 November 2007

Abstract

Transmissible spongiform encephalopaties (TSEs) or prion diseases develop as central nervous system (CNS) disorders characterized by extremely long incubation periods. Although TSEs do not go along with inflammatory infiltrates and/or antibody production against the prion protein (PrP^{Sc}), the immune system plays an important role in pathogenesis as long as different lymphoid organs (Peyer's patches, lymph nodes and spleen) may facilitate the accumulation and further spread of prions after peripheral exposure. In this work we investigated the changes in lymphoid and dendritic cell (DC) populations as well as the implications of different cytokines during disease progression after experimental oral inoculation of prions in a transgenic mouse model. At different days post-inoculation (dpi), T and B lymphocytes and DC populations from lymphoid organs, blood and brain were analyzed by flow cytometry and immunohistochemistry. Besides time related variations in lymphoid cell numbers due to the aging of the animals significant changes related with the infection were found in mesenteric lymph nodes, peripheral blood leukocytes (PBLs) as well as in spleen, affecting the CD4/CD8 ratio. In contrast, little or no variation was detected in Peyer's Patches or in thymus either associated with aging or the infection status. At individual time points significant differences between infected and control mice were seen in the CD8, CD4 and DC populations, with less evidence of differences in the B cell compartment. Finally, a pro-inflammatory phenotype occurred at early times in the spleen, where the levels of lymphotoxin-β mRNA were found augmented with respect to controls. Altogether, these results suggest that normal regulation of lymphocyte populations becomes altered along the progression of a prion infection.

Keywords: Prion infection; Lymphocyte homeostasis; T cell ratio

1. Introduction

Prion disease including Creutzfeld–Jakob disease (CJD), bovine spongiform encephalopathy (BSE) and scrapie, are fatal neurodegenerative disorders that can be transmissible. The misfolding of the host prion protein (PrP^{C}) favours the nucleation of protease-resistant aggregates (PrP^{Sc}) and subsequent accumulation in the Central Nervous System (CNS). Aggregation seems to be an irreversible phenomenon which, in turn, facilitates the conversion of new PrP^{C} molecules into PrP^{Sc}. Since the first BSE epizootic outbreak, the potential spread to other farm animals was a matter of concern and several transgenic (Tg) mouse models has been generated in an attempt to understand the molecular events governing the interspecies barrier. Among these, a Tg mouse model overexpressed the

* Corresponding author. Tel.: +34 91 620 23 00; fax: +34 91 620 22 47.
E-mail address: brun@inia.es (A. Brun).
[1] Present address: Plum Island Animal Disease Center, North Atlantic Area, Agricultural Research Service, U.S. Department of Agriculture, Greenport, New York 11944, USA.

0165-2427/$ – see front matter
doi:10.1016/j.vetimm.2007.11.013

porcine PrP^C protein ($poPrP^C$). The intracerebral administration of BSE prions to this mouse transgenic model successfully transformed $poPrP^C$ into $poPrP^{Sc}$ aggregates (Castilla et al., 2004). The newly generated prion retained BSE-like properties within a PrP porcine primary sequence.

The inoculation route of prions greatly determines the length of the incubation times. Whereas intracerebral routes accelerates prion replication in the CNS, peripheral routes such as intraperitoneal or oral routes delay PrP^{Sc} accumulation in the brain (Mabbott et al., 2000; Race et al., 2000; Prinz et al., 2003), and can even produce subclinical diseases (Thackray et al., 2003). It is believed that prions peripherally administered first encounter lymphoid tissues before spreading through the neural tissues (Klein et al., 1997; Heggebo et al., 2000). Indeed, a certain degree of replication in the lymphoid compartment seems to be required for a successful neuroinvasion (McBride et al., 2001). Knowing whether lymphoid tissues tackle or boost neuroinvasion is of paramount importance for understanding prion pathogenesis and for designing intervention strategies.

In spite of the implication of lymphoid cell populations in pathogenesis, a ''conventional'' inflammatory response has not been demonstrated in prion diseases (Mabbott and Bruce, 2001; Aguzzi, 2003; Aguzzi et al., 2003; Aguzzi and Heikenwalder, 2005). After oral inoculation of scrapie prions in mice it was shown early accumulation in the Peyer's Patches and mesenteric lymph nodes (Mabbott and Bruce, 2003; Prinz et al., 2003). Once reached the first lymphoid compartment, the prion protein can be found in these tissues depending on host factors and/or the type (strain) of prion (Foster et al., 2001; Wadsworth et al., 2001; Glatzel et al., 2003; Terry et al., 2003). Subsequently, efficient prion replication seems to be the key factor for peripheral spread and neuroinvasion (Klein et al., 1997) for which PrP^C expression in lymphoid cells, but not in B cells (Klein et al., 1998; Montrasio et al., 2001), is an essential requirement. The role of B cells seems to be related to the induction of the maturation state of follicular dendritic cells (FDC) (Klein et al., 1997; Montrasio et al., 2001; Aucouturier and Carnaud, 2002; Aguzzi and Heikenwalder, 2005), which express high amounts of surface PrP^C, by means of the proinflammatory cytokine LTα/β related to the TNF superfamily (Aguzzi and Heikenwalder, 2005).

In order to gain insights into the pathogenesis of a porcine-adapted BSE prion, we inoculated Tg mice expressing porcine prion protein (poTg001 mice) through the oral route and examinated immune cell populations along the course of the infection. We observed that the relative percentages of T and B lymphocytes varied along time in different lymphoid tissues and that these changes were different between prion inoculated and control mice groups, supporting the relevance of the immune system in prion pathogenesis. In addition, reduced number of DCs was found mainly in the spleen and Peyer's Patches of infected mice with respect to controls. Moreover, upregulation of pro-inflammatory cytokines occurred concomitantly to the variation in lymphoid cell numbers. Although the precise physiologic role of these cell fluctuations remains unknown, the data presented here are indicative of an altered homeostatic pattern at the cellular level in response to prion infection.

2. Materials and methods

2.1. Animals and TSE agent strains

The experiments were performed in poTg001 transgenic mice, expressing four fold the levels of porcine PrP^C observed in pig brain homogenates, which were generated in B6CBA/129 OLA genetic background as described (Castilla et al., 2004). The porcine-adapted BSE strain (PoTgBSE-4x) is derived from the fourth passage in poTg001 mice of a pool of material from 49 BSE-infected cattle brains supplied by the Veterinary Laboratory Agency (VLA) (New Haw, Addlestone, Surrey, UK) and characterized previously (Castilla et al., 2003). Brain homogenates (10% w/v or 20% w/v) in sterile Ca^{2+} and Mg^{2+}-free PBS or in lipid emulsion were prepared by mechanical homogenization (OMNI International, Warrenton, VA). To minimize the risk of bacterial infection, the inoculum was preheated for 10 min at 70 °C before its use in mice. All experiments with live animals were performed under the guidelines of the European Community (Directive 86/609/EEC) and were approved by the site ethical review committee.

2.2. Oral inoculation of mice and sampling material

In order to resemble the natural conditions of food intake, mice were orally inoculated with 100 μl of 20% brain homogenate in a lipid emulsion for parenteral nutrition (20% soya oil, 1.2% egg lecithin and 2.5% glycerol in water) as described (Maignien et al., 1999). Briefly, the mice were keened to drink a palatable emulsion in individual cages equipped with a liquid

delivery system (consisting of a microcentrifuge tube pierced with a 3 mm hole) before being inoculated. Consumption of the infectious preparations was carefully monitored; in all experiments described here, the mice ingested the whole inoculum within a period of 25 min. poTg001 mice ($n = 42$) were inoculated with 400 μl of a 20% PoTgBSE-4x in lipidic injectable emulsion. Control mice were fed with 400 μl of a 20% healthy (PrP^{Sc}-free) brain homogenate in lipidic emulsion ($n = 32$). Another set of mice ($n = 21$) was fed with 100 μl of the lipidic emulsion alone. Mice were bled and sacrificed under perfusion with PBS in batches of 6 inoculated, 4 control animals inoculated with healthy brain homogenate and 3 control animals fed with the lipidic emulsion alone. At 15, 25, 50, 100, 250, 300 and 400 days post-inoculation. Different organs (brain, spleen, thymus, mesenteric lymph nodes and Peyeŕs patches) were harvested. Each organ was split in two halves and used either for histopathological or FACS analysis.

2.3. Histopathology and immunohistochemistry

Brains were fixed in 10% formaline and routinely prepared for histochemical analyses and for PrP^{Sc} detection. Stained sections from medulla oblongata at the level of the obex and the pontine area, cerebellum, diencephalon, including the thalamus, hippocampus and cerebral cortex were examinated. The avidin–biotin–peroxidase complex (Vectastain ABC kit elite, Vector) technique was used for the immunohistochemical detection (IHC) of PrP^{Sc}, as described previously (Castilla et al., 2003). Tissue sections were pretreated with proteinase K and then incubated overnight at 4 °C with primary 2A11 mAb (Brun et al., 2004) diluted 1:400 in PBS. The slides were then incubated with biotinylated goat anti-mouse IgG (Dako Glostrup, Denmark), diluted 1:20 in 10% normal goat serum (Sigma Chemical Company, Dorset, Gran Bretaña). Immunoreactivity was detected with avidin-peroxidase (Dako EnVision+ System, HRP-DAB). The slides were counterstained with Harris' hematoxylin for 1 min, dehydrated and routinely mounted. Specific primary antibody was replaced by PBS or preimmune mouse serum in tissue sections used as negative controls.

Lymphoid organs were fixed in Zinc solution (20 mM Zinc Acetate, 40 mM Zinc Chloride, 3 mM Calcium Acetate in Tris buffer, pH 6.5). The alkaline–phosphatase complex (Pierce, Bonn, Germany) technique was used for the IHC detection of different types of lymphocytes ($CD4^+$, $CD8^+$ and $B220^+$ cells) using rat anti-mouse CD4, rat anti-mouse CD8 and rat anti-mouse CD45RA/B220 monoclonal antibodies (all from Pharmingen, San José, CA, USA) diluted at 1.100. After deparaffination and rehydration, tissue sections were incubated overnight at 4 °C with primary monoclonal antibody. After incubation with secondary anti-rat IgG (Pharmingen, San José, CA, USA) detection was carried out with 0.02% Fast Red chromogen (Fast Red Sustrate Packz, Lab Biogenex, USA) diluted in Tris–naftol buffer, counterstained and mounted with ImmuMount® (Shandon Inc., Dreieich, Germany) without previous dehydration. As for brain tissue, specific primary antibody was replaced by PBS or preimmune mouse serum in tissue sections used as negative controls.

2.4. Isolation of lymphoid cells, peripheral blood lymphocytes (PBLs) and flow cytometry analysis

Lymphoid organs were obtained from poTg001 inoculated or control mice and single cell suspensions were then obtained by mechanical disruption. Cells were pelleted by centrifugation and resuspended in staining buffer (PBS containing 2% (v/v) fetal bovine serum and 0.2% (w/v) NaN_3) for flow cytometry. PBLs were isolated from peripheral blood of inoculated or control mice as described (Sevilla et al., 2000). Briefly, fresh heparinized peripheral blood was mixed with an equal volume of phosphate-buffered saline (PBS). Ficoll-Hypaque (1.007 g/l) was layered underneath the blood/PBS mixture and centrifuged 30 min at $900 \times g$. The mononuclear cell layer was transferred to another tube, washed, and cell viability determined by Trypan Blue exclusion. To analyze the expression of cell surface molecules, we used monospecific antibodies, fluorochrome dyes, and flow cytometry. The antibodies used were rat anti-mouse CD8α-PerCp, rat anti-mouse CD4-FITC, rat anti-mouse B220-APC, rat anti-mouse CD3-FITC, and rat anti-mouse CD11c-PE (all from BD Pharmingen, San Jose, CA, USA). Cells were acquired using a FACSCalibur flow cytometer (Becton Dickinson, Franklin Lakes, NJ, USA). Dead cells were excluded on the basis of forward and side light scatter. Data were analyzed with FlowJo (Tree Star, San Francisco, CA, USA) and CellQuest software (Becton Dickinson).

2.5. RNAse protection assay (RPA)

Total RNA was isolated from whole mesenteric lymph node or spleen homogenates using Tri-Reagent (Molecular Research Center, Cincinnati, OH, USA). RNA was extracted with chloroform followed by

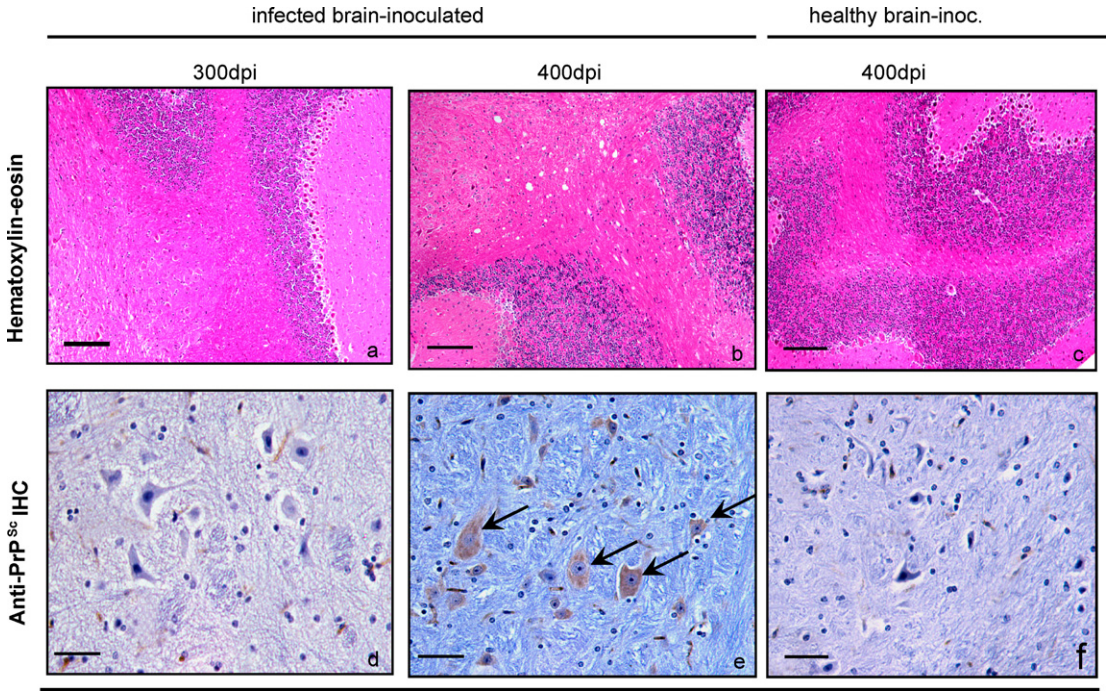

Fig. 1. Histopathological findings in the central nervous system (CNS) of poTg001 inoculated mice. Hematoxylin–eosin staining (magnification 100×) of the cerebellum from a poTg001-inoculated mouse with infected brain material at 300 dpi (a) and 400 dpi (b), or from mouse inoculated with PrP^{Sc}-free brain material at 400 dpi (c). Scale bars: 200 μm. Immunostaining (magnification 400×) of the obex from a poTg001 inoculated with infected brain material at 300 dpi (d) and 400 dpi (e), or from mouse inoculated with PrP^{Sc}-free brain-material at 400 dpi (f). Intraneuronal PrP^{res} deposits in the neuronal nuclei of the brain stem are shown with arrows. Scale bars: 50 μm.

isopropanol precipitation and washing with ethanol. Twenty micrograms of total RNA was used for hybridization with a ^{32}P-UTP-labelled multitemplate set containing specific probes for LTα, LTβ, TNF, IL-6, INFγ, IFNβ, TGFβ1, TGFβ2, TGFβ3 and MIF (Riboquant, mCK-3b; BD PharMingen). The RPA was conducted according to the manufacturer's guidelines. The resulting analytical acrylamide gel was scanned using a STORM-860 PhosphorImager (Molecular Dynamics, Sunnyvale, CA), and the intensity of bands corresponding to protected mRNA was quantified using ImageQuant image analysis software (Molecular Dynamics). For each tissue analyzed, sample values were normalized against the ribosomal protein L32 or GADPH housekeeping genes.

2.6. Statistical analyses

The statistical analysis was performed with the general lineal model (GLM) procedure of SAS (SAS/STATk, 1999. Release 8.2. SAS Institute Inc., Cary NC, USA) using the following mixed ANOVA model: $\underline{X}_{ijk} = \mu + t_i + i_j + (t \times i)_{ij} + e_{ijk}$, where μ, mean; t, time post-inoculation, i, inoculum; $t \times i$, interaction; e, standard error. As post hoc tests, Duncan's multiple-range comparison test or least significant difference test (LSD) were used to compare means from infected and control samples at equivalent time points.

3. Results

3.1. Susceptibility of poTg mice to porcine-adapted prion

At 300 days post-inoculation all mice showed signs of neurological dysfunction although no pathological lesions such as vacuolation, gliosis or PrP^{Sc} deposits were observed in limited tissue sections by histological analysis (Fig. 1a and d). However, at 400 dpi poTg001 mice (6/6) showed vacuolation mainly in the neuropil, cromatolysis, and neuronophagia and neuronal lose with gliosis essentially affecting the cerebellum (Fig. 1b) and the brainstem. Immunohistochemical staining showed intraneuronal PrP^{Sc} in the brainstem in the form of diffuse granular deposits spread along the neuronal perikarya in 100% of analyzed mice (Fig. 1e). These pathological findings were not evident at 400 dpi in control animals, either animals inoculated with healthy brain homogenates (Fig. 1c and f) or mice fed with lipidic injectable emulsion alone (data not shown).

Table 1
Degrees of freedom, mean squares, *F*-values and significance of time and type of inoculum affecting lymphoid cell numbers in different tissues

Tissue	Source of variation	CD4			CD8			CD4/CD8 ratio			B220			B/T cell ratio		
		d.f.	Mean square	*F*	d.f.	Mean square	*F*	d.f.	Mean square	*F*	d.f.	Mean square	*F*	d.f.	Mean square	*F*
Spleen	Time	4	56.9	9.93***	3	141.1	22.52***	3	0.104	14.66***	4	229.9	8.94***	3	2.772	5.12*
	Inoculum	1	5.4	0.95	1	2.57	0.41	1	0.006	0.91	1	1.9	0.08	1	0.364	0.67
	$t \times i$	4				24.8	3.97*		0.120	16.88***						
Mesenteric lymph node	Time	4	185.4	7.24***	4	35.8	6.55**	4	0.111	2.26	4	59.7	1.73	4	0.029	2.79
	Inoculum	1	24.6	0.96	1	17.2	3.15	1	0.218	4.42*	1	32.9	0.95	1	0.001	0.11
	$t \times i$	4	112.7	4.40*										4	0.052	5.01**
PBLs	Time	4	632.7	5.59**	4	190.6	8.89***	4	24.037	98.32***	4	250	2.41	4	0.045	0.67
	Inoculum	1	251.8	2.23	1	19.1	0.89	1	12.966	53.04***	1	63.0	0.61	1	0.219	3.23
	$t \times i$				4	157.6	7.35***	4	14.960	61.19***	4	101.4	2.93*			
Thymus	Time	4	19.9	3.92*	4	0.8	0.53	4	1.094	1.12	n.a.	n.a.	n.a.	n.a.	n.a.	n.a.
	Inoculum	1	3.0	6.60	1	0.7	0.49	1	0.438	0.45	n.a.	n.a.	n.a.	n.a.	n.a.	n.a.
Peyer's Patches	Time	4	91.4	0.62	4	48.2	0.57	4	0.531	1.36	4	521.3	2.61	4	0.724	1.48
	Inoculum	1	62.1	0.42	1	55.2	0.65	1	0.829	2.13	1	20.2	0.10	1	0.371	0.76

Values for significant interactions ($t \times i$) are also shown. *$P < 0.05$, **$P < 0.01$ and ***$P < 0.001$; n.a., not applicable.

These data indicated that poTg001 mice were susceptible to the oral infection with poTgBSE-4x and, therefore, a suitable model for our study.

3.2. Analysis of lymphocyte cell populations after oral prion infection

To gain insights about the status of T and B cell populations during PrP infection, flow cytometry analysis was used to quantify cell numbers at different times post-inoculation. Suspensions of single cells prepared from individual thymus (T), mesenteric lymph nodes (MLN), Peyer's patches (PP) and spleen (S) were labelled with specific monoclonal antibodies anti-CD4, anti-CD8 and anti-B220 coupled to a fluorochrome probe. In addition, peripheral blood lymphocytes (PBLs) were obtained by Ficoll gradient purification. To identify variation in tissue specific lymphoid cell numbers we used a general linear model (GLM) considering both the inoculum (infection) and time (aging) as the possible sources of variation. Thus we could identify those tissues in which variations in cell numbers occurred with statistical significance (Table 1). Thus, the age of the animals was found as an important source of variation in all tissues studied but not in PP and T, which remained constant along the course of time. Variation attributed to the infection was restricted to the T-cell subset in S, MLN, and PBLs. In contrast, B-cell number variability was found only to be significant in S. In this organ, the variation related with the infection affected both the $CD4^+$ and $CD8^+$ cell populations as well as the $CD4^+/CD8^+$ cell ratio for which a highly significant interaction effect was observed for time and type of inoculum (Table 1). This effect was restricted to late time points. Direct comparison between inoculated and control groups at 250 dpi revealed a significant decrease in the $CD8^+$ subset as well as an increase in the $CD4^+$ cells in prion infected mice with respect to mock infected animals (Fig. 2). Thus, the spleen $CD4^+/CD8^+$ ratio was higher in the infected mice (1.16 ± 0.05, mean $\pm$ S.D.) than in PrP^{Sc}-free brain inoculated controls (0.74 ± 0.07). These alterations in the number of $CD4^+$ and $CD8^+$ cells were also confirmed by IHC (Fig. 3b, E and K). On the other hand, the spleen maintained constant B/T cell ratios along the course of the infection with the exception of 250 dpi where a reduction in the number of B-cells was observed in both experimental groups (Fig. 2). In MLN, variations also affected mostly the T-cell subset without affecting the $CD4^+/CD8^+$ ratio, but significant differences in the number of B-cells were detected at early times (15–25 dpi) among inoculation groups. Thus an increased $B220^+$ subset in prion inoculated mice is observed at 15 dpi whereas reaches near control levels at 25 dpi. These differences could be also seen by IHC analysis (Fig. 3a, A–D). On the other hand, the T-cell compartment was also affected with a reduction in the number of $CD8^+$ at 15 dpi, observed by IHC (Fig. 3a, G and H), and a significant increase in the $CD4^+$ cell counts at 25 dpi (Fig. 2). The thymic microarchitecture remained unaffected when observed by IHC (data not shown), in agreement with the constant lymphocyte number recorded at any time point. In PP, differences were only found between mice groups and

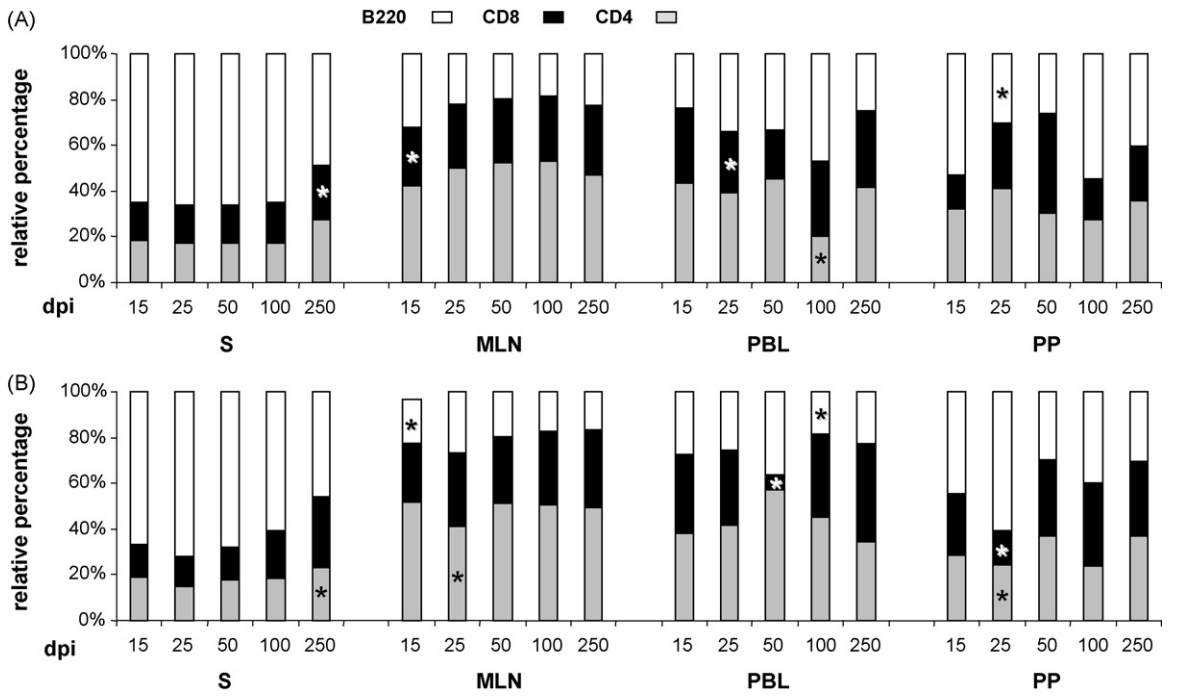

Fig. 2. Evolution of B and T-cell populations during poBSE prion infection in mice. Relative percentages of B and T cells in spleen (S), mesenteric lymph nodes (MLN), peripheral blood leukocytes (PBL) and Peyer's Patches (PP) at different times post-inoculation in mice inoculated with the infected brain material (A) or in control animals inoculated with healthy brain material (B). Asterisks denote a significant decrease in cell numbers with respect to the corresponding control or infected group.

restricted to 25 dpi, due to significant $CD8^+$ and $CD4^+$ cell expansion at 25 dpi (Fig. 2). The highest fluctuation in the number of lymphocytes along the course of the infection was found in circulating PBLs. The T-cell ratios were influenced both by kinetics and also by the type of inoculum used, with marked interaction significances (Table 1). The kinetics of the cell numbers differed notably between infected and control mice (Fig. 2). In control mice, while the B/T cell ratio showed no significant variation along time, the $CD4^+/CD8^+$ cell ratio showed a marked step rise with a further decrease at some point between 50 and 100 dpi. In contrast, infected mice displayed altered T-cell ratios in all time points analyzed until later times after inoculation, where the cell ratios were indistinguishable from controls. In spite of the altered T-cell ratios, the B/T cell ratio was kept constant with the only exception of the 100 dpi time point in which the $B220^+$ population showed a very significant expansion with respect to the controls. Taken together these data suggest that, upon prion infection, the homeostatic control of the lymphoid cell populations is altered at discrete time points in S, MLN and PP but in PBLs the normal pattern of lymphoid cell circulation is largely disrupted after the infection.

3.3. Analyses of dendritic cell (DC) populations after oral prion infection

The involvement of dendritic cells (DC) in TSE pathogenesis has been suggested (Huang et al., 2002), although their precise role in the aetiology of these diseases remains to be demonstrated. Due to the pivotal role of DC in encountering pathogens and mounting a successful immune response, we went to analyze the status of DC subpopulations during the progression of disease in our infection mouse model. We focused in three different DC subpopulations, all gated in $CD11c^+$ cells, which include $CD8^-$ (myeloid) and $CD8^+$ (lymphoid) DCs and plasmacytoid DCs, expressing the CD45 isoform (B220) normally expressed by B cells. Single cell preparations were obtained from MLN, PP and S taken from individually infected mice at different dpi. These cells were stained with specific monoclonal antibodies against CD8, B220, CD11c and CD3 antibodies (see Section 2) conjugated to a fluorochrome and analyzed by FACS. Along time, significant variations in the DC population were found in all tissues analyzed with higher significance in the myeloid compartment and, to a lesser extent, for plasmacytoid cells (Table 2). Although a significant

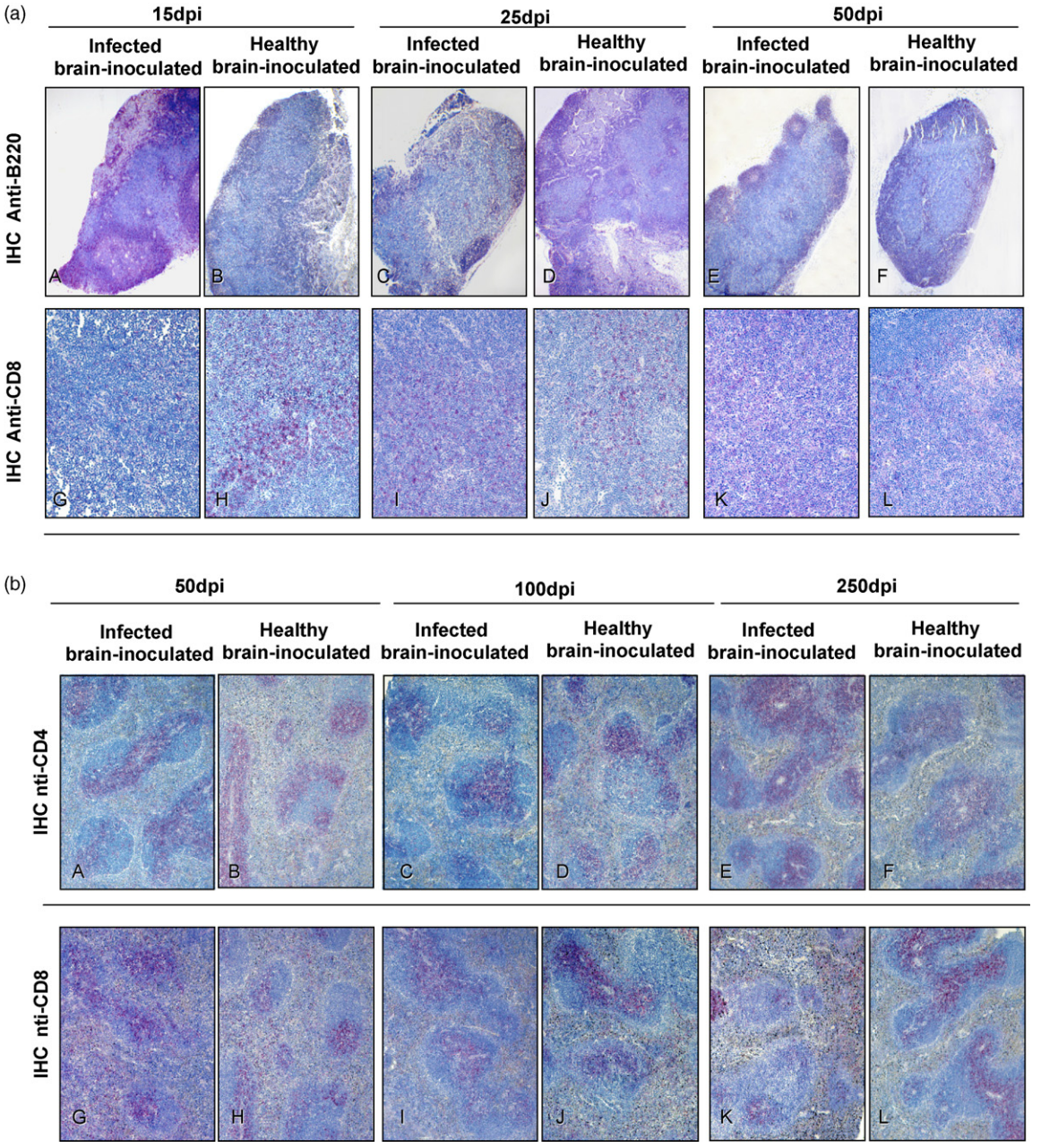

Fig. 3. Expression of CD4, CD8 and B220 molecules on lymphoid tissues. (a) B-cell (A–F, magnification 40×) or $CD8^+$ cell immunostainig (G–L, magnification 100×) of mouse mesenteric lymph nodes at different times post-inoculation. (b) Spleen immunostaining (magnification 100×) of $CD4^+$ (A–F) and $CD8^+$ (G–L) lymphocytes in samples from infected and control mice at different times post-inoculation.

level of variability, due to the aging of the animal, was found associated to these DC compartments, MLN did not show any change in these subpopulations during disease development with respect to control mice. Only at later times a significant decrease in lymphoid DC was found with respect to controls. In contrast, PP showed reduced numbers of plasmacytoid and myeloid DCs at 15 dpi with no significant changes for the lymphoid DC population (Table 2 and Fig. 4). In spleen, significant differences were found at late times (100 dpi) for both the myeloid and plasmacytoid cell subsets. Overall, the changes observed in the infected mice for the dendritic cell compartment are related with a reduction in cell numbers.

Table 2
Degrees of freedom, mean squares, *F*-values and significance of time and type of inoculum affecting dendritic cell numbers in different tissues

Tissue	Source of variation	Lymphoid DCs			Myeloid DCs			Plasmacytoid DCs		
		d.f.	Mean square	*F*	d.f.	Mean square	*F*	d.f.	Mean square	*F*
Spleen	Time	4	0.09	8.16***	4	4.60	10.41***	4	0.90	4.34*
	Inoculum	1	0.0002	0.02	1	1.12	2.55	1	0.42	2.07
	$t \times i$				4	1.61	3.64*	4	0.50	2.45
Mesenteric lymph node	Time	4	0.13	6.41**	4	7.52	9.30***	4	4.96	4.53**
	Inoculum	1	0.06	3.42	1	0.70	0.87	1	2.73	2.50
PBLs	Time	4	0.15	0.65	4	133.22	15.17***	4	21.87	35.83***
	Inoculum	1	0.37	1.49	1	0.55	0.06	1	0.85	1.40
Peyer patches	Time	4	0.37	1.03	4	58.98	13.07***	4	36.33	10.49***
	Inoculum	1	0.05	0.14	1	18.88	4.18	1	8.84	2.55

Values for significant interactions ($t \times i$) are also shown. *$P < 0.05$, **$P < 0.01$ and ***$P < 0.001$.

3.4. Expression of LTβ and TFGβ in MLN and S after oral prion infection

To characterize the activation of the immune system at the molecular level, changes in the expression profiles of a panel of cytokines were analyzed by RNA protection assay (RPA) on MLN and S tissue from infected and age-matched PrP^{Sc}-free brain inoculated mice at different dpi. The most significant alterations were seen in the anti-inflammatory cytokine transforming growth factor-β (TGFβ) and the pro-inflammatory lymphotoxin-β (LTβ) showing different kinetics in MLN and S (Fig. 5). While TGFβ showed a decreased expression at early times (15 and 50 dpi) in MLN, reaching normal values at later dpi (100 and 250 dpi), a continuous declined expression in spleen during disease progression was observed. The same pattern was found for LTβ expression in MLN. Thus, LTβ was down-

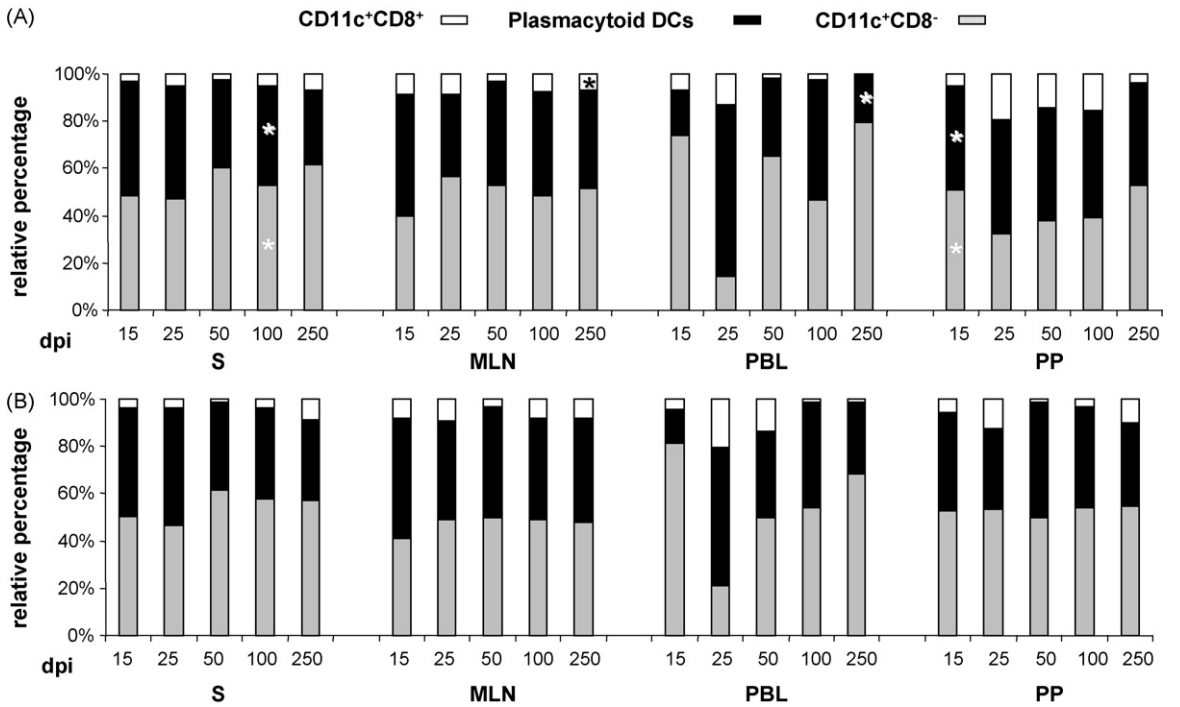

Fig. 4. Kinetic analysis of dendritic $CD11c^+$ after poBSE infection. Relative percentages of myeloid, lymphoid and plasmacytoid dendritic cells in different secondary lymphoid organs and PBLs at different times post-inoculation in mice inoculated with poBSE inoculum (A) or in control animals (B). Asterisks denote significant decrease in cell numbers with respect to the corresponding control or infected group.

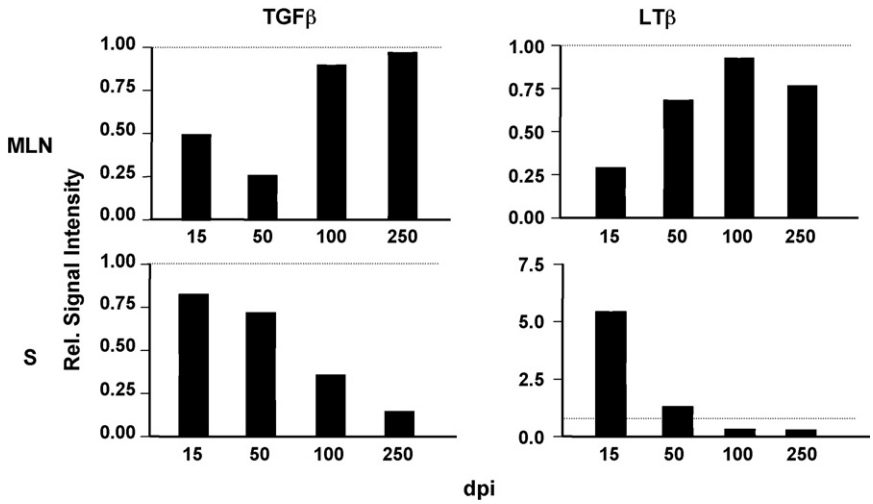

Fig. 5. Expression of TGFβ and LTβ after poBSE infection in mesenteric lymph node (MLN) and spleen (S). RPA using total RNA isolated from MLN or S homogenates of poTg100 mice at 15, 50, 100 and 200 dpi. For quantification of the relative amounts of individual mRNA species, the signal intensities were normalized against L32 and are depicted relative to the mRNA amounts expressed in PrP^{Sc}-free brain-inoculated mice. Data represent mean relative signal intensities.

regulated during early stages of disease in MLN to increase at later dpi. However in spleen, LTβ was found overexpressed (6 fold the levels found in control mice) at early times but reaching almost undetectable levels at 100–200 dpi suggesting an ongoing activation of DC needed for prion expansion.

4. Discussion

In our mouse model the homeostatic control of lymphoid cell populations resulted altered in some secondary lymphoid organs along the course of an oral prion infection. These alterations were identified in addition those related with the aging of the mice, and resulted in fluctuations in the relative numbers of B and T cells in all tissues studied but thymus. In agreement with the pathogenesis of prions, significant fluctuations are observed in PP and MLN at early times post-challenge, whereas no variation is detected in S before 250 dpi, time at which the accumulation of PrP^{Sc} in this organ has been described (Maignien et al., 1999). In contrast, the T-cell ratio was quite unbalanced in the PBL fraction, particularly at 100 dpi: while $CD8^+$ cell percentages remained unaltered, a significant decrease in $CD4^+$ T cells was coincidental with a 30% increase in B220 cell counts. Thus, blood leukocyte ratios may serve as indicators of prion propagation in other lymphoid tissues. It would be interesting to assess whether this level of altered PBL ratios could also be observed in other species and/or with different prion strains. B lymphocytes have been described as playing an important role in the pathogenesis of TSEs, specifically derived from the important role by secreting soluble citokines (TNF-α) or membrane cytokines (lymphotoxin $\alpha_1\beta_2$) (Mabbott and Bruce, 2001) promoting FDCs maturation (Fu et al., 1998; Chaplin and Fu, 1998) in lymph nodes, Peyer's patches and germinal centres of spleen. Increment of B cell numbers at late stages of infection might induce the increase in the number of mature FDCs thus facilitating spleen PrP^{Sc} accumulation (Maignien et al., 1999). On the other hand, evidence that T lymphocytes are not involved in TSEs pathogenesis came from earlier studies showing that thymectomy had no effect on incubation period disease following peripheral infection (McFarlin et al., 1971; Fraser and Dickinson, 1978), although other studies found the presence of T lymphocytes in the CNS of infected animals (Lewicki et al., 2003). In our model we did not find any thymic cellular alteration, although significant variations in the relative number of T cells where observed in other secondary lymphoid organs (spleen, Peyer's patches and mesenteric lymph nodes) and PBLs.

Several cell types have been implicated in prion spread prior to neuroinvasion. Gut epithelial M cells, which are involved in mucosal immunity (Neutra et al., 1996a,b) have shown to be implicated in prion retention (Heppner et al., 2001) and are located in the vicinity of DCs in the intestine (Defaweux et al., 2005). DCs are essential elements of the immune system due to their capacity to induce and regulate Ag-specific immune responses, allowing them to control infections caused

by different pathogens. The remarkably functional diversity of the DC system relies on the plasticity and complexity of the DC differentiation process, which leads to the generation of a large collection of DC subpopulations, endowed with specific functions. DCs can be classified in two major categories: conventional DCs (Mayordomo et al., 1997; Steinman et al., 1997) and pDCs (O'Keeffe et al., 2002; Schlecht et al., 2004), characterized by their capacity to produce large amounts of type I IFNs during viral infections (Kadowaki et al., 2000). It has been demonstrated that scrapie-infected DCs intravenously injected can propagate prions (Huang et al., 2002). These data shows the importance of understanding the possible role of DCs in prion spread and neuroinvasion and its relation with the accepted role of FDCs in the pathogenesis of TSEs (Klein et al., 2001; Mabbott and Bruce, 2001) Our results show that during disease course after oral intake of prion infected brain material, there is a general reduction in the number of DCs. At early stages of the disease (15 dpi) the reduction is shown mainly in PP. This might be indicative of a redistribution of non-lymphoid DCs in other tissue compartments that is reflected in a decreased in the number of DCs. In fact, there is replenishment (normal values by 25 dpi) of DCs from blood in lymphoid tissues. This replenishment is reflected in the reduced number of DCs in PBL at 25 dpi that are recruited to lymphoid organs. Coincidentally, we observed a decrease of $CD8^+$ cells from PBLs and $CD4^+$ cells from MLN at early times post-prion exposure, suggesting a possible role of the T cell compartment in pathogenesis. On the membrane of T cells, PrP^C molecules have been found to be associated with the TCR/CD3 complex upon engagement with MHC II/Ag peptide or anti-CD3 antibodies (Mattei et al., 2004; Ballerini et al., 2006) These and our data may suggest that DCs are activating T cells, activation that drives a general cell organization reflected in decreased cell numbers. Interestingly, normal values of DC numbers are reached by 50 dpi in all analyzed tissues. However, at later times of the disease there is again a decrease in the number of DCs in S and PBLs. At this time post-inoculation the number of T cells is also decreasing. These results suggest a role in prion pathogenesis, although additional studies need to be done to further elucidate the role of DC-T cell interaction in prion infectivity.

Immune mediated inflammatory responses have never been evident for prion diseases. Theoretically, a feasible explanation for the apparent lack of inflammation relies in the immunological tolerance of the host, which may recognise the prion (PrP^{Sc}) as a self-antigen. However an "atypical" inflammatory response can be observed in many TSEs (Perry et al., 2002). With some exceptions related to specific prion strains, the lymphoid compartment plays a key role retaining and facilitating prion infectivity after ingestion or peripheral exposure (Aguzzi and Heikenwalder, 2005). Our data suggest that an atypical inflammatory response takes place most noticeable at early times post-infection. The levels of the anti-inflammatory TGFβ appeared down-regulated at early times in MLN and at late times in S whereas at very early times the proinflamatory LTβ levels were upregulated. Since the role of TGFβ in peripheral tissues could be related with the induction of T regulatory cell subsets, low levels of this cytokine can be associated with a pro-inflammatory phenotype On the other hand the expression of LTβ can be related with the production of homeostatic chemokines produced by FDCs (Ansel et al., 2000) and the maturation of FDCs itself, providing the essential organization of the lymphoid follicles. Thus the initial inflammatory response triggered by the host after prion infection can facilitate prion replication, as long as it has been demonstrated that animals lacking LTβ did not accummulate either PrP^{Sc} or infectivity following prion inoculation (Aguzzi and Heikenwalder, 2006). Whether the immune cell-mediated prion spread and the atypical inflammatory response are related phenomena deserves further attention.

Acknowledgements

The authors thank Juan M. Torres for supplying the poTg001 mouse model and the inoculum used in this work. FD-S was a fellowship of INIA. This work was supported by Spanish national grants RC01-0605, EET2002-05168 and AGL2004-00499 from Ministry of Education and Science (Spain).

References

Aguzzi, A., 2003. Prions and the immune system: a journey through gut, spleen, and nerves. Adv. Immunol. 81, 123–171.

Aguzzi, A., Heikenwalder, M., 2005. Prions, cytokines, and chemokines: a meeting in lymphoid organs. Immunity 22, 145–154.

Aguzzi, A., Heikenwalder, M., 2006. Pathogenesis of prion diseases: current status and future outlook. Nat. Rev. Microbiol. 4, 765–775.

Aguzzi, A., Heppner, F.L., Heikenwalder, M., Prinz, M., Mertz, K., Seeger, H., Glatzel, M., 2003. Immune system and peripheral nerves in propagation of prions to CNS. Br. Med. Bull. 66, 141–159.

Ansel, K.M., Ngo, V.N., Hyman, P.L., Luther, S.A., Forster, R., Sedgwick, J.D., Browning, J.L., Lipp, M., Cyster, J.G., 2000. A chemokine-driven positive feedback loop organizes lymphoid follicles. Nature 406, 309–314.

Aucouturier, P., Carnaud, C., 2002. The immune system and prion diseases: a relationship of complicity and blindness. J. Leukoc. Biol. 72, 1075–1083.

Ballerini, C., Gourdain, P., Bachy, V., Blanchard, N., Levavasseur, E., Gregoire, S., Fontes, P., Aucouturier, P., Hivroz, C., Carnaud, C., 2006. Functional implication of cellular prion protein in antigen-driven interactions between T cells and dendritic cells. J. Immunol. 176, 7254–7262.

Brun, A., Castilla, J., Ramirez, M.A., Prager, K., Parra, B., Salguero, F.J., Shiveral, D., Sanchez, C., Sanchez-Vizcaino, J.M., Douglas, A., Torres, J.M., 2004. Proteinase K enhanced immunoreactivity of the prion protein-specific monoclonal antibody 2A11. Neurosci. Res. 48, 75–83.

Castilla, J., Gutierrez Adan, A., Brun, A., Pintado, B., Ramirez, M.A., Parra, B., Doyle, D., Rogers, M., Salguero, F.J., Sanchez, C., Sanchez-Vizcaino, J.M., Torres, J.M., 2003. Early detection of PrP(res) in BSE-infected bovine PrP transgenic mice. Arch. Virol. 148, 677–691.

Castilla, J., Gutierrez-Adan, A., Brun, A., Doyle, D., Pintado, B., Ramirez, M.A., Salguero, F.J., Parra, B., Segundo, F.D., Sanchez-Vizcaino, J.M., Rogers, M., Torres, J.M., 2004. Subclinical bovine spongiform encephalopathy infection in transgenic mice expressing porcine prion protein. J. Neurosci. 24, 5063–5069.

Chaplin, D.D., Fu, Y., 1998. Cytokine regulation of secondary lymphoid organ development. Curr. Opin. Immunol. 10, 289–297.

Defaweux, V., Dorban, G., Demonceau, C., Piret, J., Jolois, O., Thellin, O., Thielen, C., Heinen, E., Antoine, N., 2005. Interfaces between dendritic cells, other immune cells, and nerve fibres in mouse Peyer's patches: potential sites for neuroinvasion in prion diseases. Microsci. Res. Tech. 66, 1–9.

Foster, J.D., Parnham, D.W., Hunter, N., Bruce, M., 2001. Distribution of the prion protein in sheep terminally affected with BSE following experimental oral transmission. J. Gen. Virol. 82, 2319–2326.

Fraser, H., Dickinson, A.G., 1978. Studies of the lymphoreticular system in the pathogenesis of scrapie: the role of spleen and thymus. J. Comp. Pathol. 88, 563–573.

Fu, Y.X., Huang, G., Wang, Y., Chaplin, D.D., 1998. B lymphocytes induce the formation of follicular dendritic cell clusters in a lymphotoxin alpha-dependent fashion. J. Exp. Med. 187, 1009–1018.

Glatzel, M., Abela, E., Maissen, M., Aguzzi, A., 2003. Extraneural pathologic prion protein in sporadic Creutzfeldt–Jakob disease. N. Engl. J. Med. 349, 1812–1820.

Heggebo, R., Press, C.M., Gunnes, G., Lie, K.I., Tranulis, M.A., Ulvund, M., Groschup, M.H., Landsverk, T., 2000. Distribution of prion protein in the ileal Peyer's patch of scrapie-free lambs and lambs naturally and experimentally exposed to the scrapie agent. J. Gen. Virol. 81, 2327–2337.

Heppner, F.L., Christ, A.D., Klein, M.A., Prinz, M., Fried, M., Kraehenbuhl, J.P., Aguzzi, A., 2001. Transepithelial prion transport by M cells. Nat. Med. 7, 976–977.

Huang, F.P., Farquhar, C.F., Mabbott, N.A., Bruce, M.E., MacPherson, G.G., 2002. Migrating intestinal dendritic cells transport PrP(Sc) from the gut. J. Gen. Virol. 83, 267–271.

Kadowaki, N., Antonenko, S., Lau, J.Y., Liu, Y.J., 2000. Natural interferon alpha/beta-producing cells link innate and adaptive immunity. J. Exp. Med. 192, 219–226.

Klein, M.A., Frigg, R., Flechsig, E., Raeber, A.J., Kalinke, U., Bluethmann, H., Bootz, F., Suter, M., Zinkernagel, R.M., Aguzzi, A., 1997. A crucial role for B cells in neuroinvasive scrapie. Nature 390, 687–690.

Klein, M.A., Frigg, R., Raeber, A.J., Flechsig, E., Hegyi, I., Zinkernagel, R.M., Weissmann, C., Aguzzi, A., 1998. PrP expression in B lymphocytes is not required for prion neuroinvasion. Nat. Med. 4, 1429–1433.

Klein, M.A., Kaeser, P.S., Schwarz, P., Weyd, H., Xenarios, I., Zinkernagel, R.M., Carroll, M.C., Verbeek, J.S., Botto, M., Walport, M.J., Molina, H., Kalinke, U., Acha-Orbea, H., Aguzzi, A., 2001. Complement facilitates early prion pathogenesis. Nat. Med. 7, 488–492.

Lewicki, H., Tishon, A., Homann, D., Mazarguil, H., Laval, F., Asensio, V.C., Campbell, I.L., DeArmond, S., Coon, B., Teng, C., Gairin, J.E., Oldstone, M.B., 2003. T cells infiltrate the brain in murine and human transmissible spongiform encephalopathies. J. Virol. 77, 3799–3808.

Mabbott, N.A., Bruce, M.E., 2001. The immunobiology of TSE diseases. J. Gen. Virol. 82, 2307–2318.

Mabbott, N.A., Bruce, M.E., 2003. Prion disease: bridging the spleen–nerve gap. Nat. Med. 9, 1463–1464.

Mabbott, N.A., Mackay, F., Minns, F., Bruce, M.E., 2000. Temporary inactivation of follicular dendritic cells delays neuroinvasion of scrapie. Nat. Med. 6, 719–720.

Maignien, T., Lasmezas, C.I., Beringue, V., Dormont, D., Deslys, J.P., 1999. Pathogenesis of the oral route of infection of mice with scrapie and bovine spongiform encephalopathy agents. J. Gen. Virol. 80 (Pt 11), 3035–3042.

Mattei, V., Garofalo, T., Misasi, R., Circella, A., Manganelli, V., Lucania, G., Pavan, A., Sorice, M., 2004. Prion protein is a component of the multimolecular signaling complex involved in T cell activation. FEBS Lett. 560, 14–18.

Mayordomo, J.I., Zorina, T., Storkus, W.J., Zitvogel, L., Garcia-Prats, M.D., DeLeo, A.B., Lotze, M.T., 1997. Bone marrow-derived dendritic cells serve as potent adjuvants for peptide-based antitumor vaccines. Stem Cells 15, 94–103.

McBride, P.A., Schulz-Schaeffer, W.J., Donaldson, M., Bruce, M., Diringer, H., Kretzschmar, H.A., Beekes, M., 2001. Early spread of scrapie from the gastrointestinal tract to the central nervous system involves autonomic fibers of the splanchnic and vagus nerves. J. Virol. 75, 9320–9327.

McFarlin, D.E., Raff, M.C., Simpson, E., Nehlsen, S.H., 1971. Scrapie in immunologically deficient mice. Nature 233, 336.

Montrasio, F., Cozzio, A., Flechsig, E., Rossi, D., Klein, M.A., Rulicke, T., Raeber, A.J., Vosshenrich, C.A., Proft, J., Aguzzi, A., Weissmann, C., 2001. B lymphocyte-restricted expression of prion protein does not enable prion replication in prion protein knockout mice. Proc. Natl. Acad. Sci. U.S.A. 98, 4034–4037.

Neutra, M.R., Frey, A., Kraehenbuhl, J.P., 1996a. Epithelial M cells: gateways for mucosal infection and immunization. Cell 86, 345–348.

Neutra, M.R., Pringault, E., Kraehenbuhl, J.P., 1996b. Antigen sampling across epithelial barriers and induction of mucosal immune responses. Annu. Rev. Immunol. 14, 275–300.

O'Keeffe, M., Hochrein, H., Vremec, D., Caminschi, I., Miller, J.L., Anders, E.M., Wu, L., Lahoud, M.H., Henri, S., Scott, B., Hertzog, P., Tatarczuch, L., Shortman, K., 2002. Mouse plasmacytoid cells: long-lived cells, heterogeneous in surface phenotype and function, that differentiate into CD8(+) dendritic cells only after microbial stimulus. J. Exp. Med. 196, 1307–1319.

Perry, V.H., Cunningham, C., Boche, D., 2002. Atypical inflammation in the central nervous system in prion disease. Curr. Opin. Neurol. 15, 349–354.

Prinz, M., Huber, G., Macpherson, A.J., Heppner, F.L., Glatzel, M., Eugster, H.P., Wagner, N., Aguzzi, A., 2003. Oral prion infection

requires normal numbers of Peyer's patches but not of enteric lymphocytes. Am. J. Pathol. 162, 1103–1111.

Race, R., Oldstone, M., Chesebro, B., 2000. Entry versus blockade of brain infection following oral or intraperitoneal scrapie administration: role of prion protein expression in peripheral nerves and spleen. J. Virol. 74, 828–833.

Schlecht, G., Garcia, S., Escriou, N., Freitas, A.A., Leclerc, C., Dadaglio, G., 2004. Murine plasmacytoid dendritic cells induce effector/memory CD8+ T-cell responses in vivo after viral stimulation. Blood 104, 1808–1815.

Sevilla, N., Kunz, S., Holz, A., Lewicki, H., Homann, D., Yamada, H., Campbell, K.P., de La Torre, J.C., Oldstone, M.B.., 2000. Immunosuppression and resultant viral persistence by specific viral targeting of dendritic cells. J. Exp. Med. 192, 1249–1260.

Steinman, R.M., Pack, M., Inaba, K., 1997. Dendritic cells in the T-cell areas of lymphoid organs. Immunol. Rev. 156, 25–37.

Terry, L.A., Marsh, S., Ryder, S.J., Hawkins, S.A., Wells, G.A., Spencer, Y.I., 2003. Detection of disease-specific PrP in the distal ileum of cattle exposed orally to the agent of bovine spongiform encephalopathy. Vet. Rec. 152, 387–392.

Thackray, A.M., Klein, M.A., Bujdoso, R., 2003. Subclinical prion disease induced by oral inoculation. J. Virol. 77, 7991–7998.

Wadsworth, J.D., Joiner, S., Hill, A.F., Campbell, T.A., Desbruslais, M., Luthert, P.J., Collinge, J., 2001. Tissue distribution of protease resistant prion protein in variant Creutzfeldt–Jakob disease using a highly sensitive immunoblotting assay. Lancet 358, 171–180.